Towards Pre-alignment of Near-infrared Iris Images

P. Drozdowski[1,2] • C. Rathgeb[1] • H. Hofbauer[3] • J. Wagner[1] • A. Uhl[3] • C. Busch[1]

[1]da/sec - Biometrics and Internet Security Research Group, Hochschule Darmstadt, Germany,
{pawel.drozdowski,christian.rathgeb,johannes.wagner,christoph.busch}@h-da.de
[2]Norwegian Biometrics Laboratory, NTNU, Gjøvik, Norway
[3]Multimedia Signal Processing and Security Lab, University of Salzburg, Austria, {hhofbaue,uhl}@cosy.sbg.ac.at

Abstract

The necessity of biometric template alignment imposes a significant computational load and increases the probability of false positive occurrences in biometric systems. While for some modalities, automatic pre-alignment of biometric samples is utilised, this topic has not yet been explored for systems based on the iris.

This paper presents a method for pre-alignment of iris images based on the positions of automatically detected eye corners. Existing work in the area of automatic eye corner detection has hitherto only involved visible wavelength images; for the near-infrared images, used in the vast majority of current iris recognition systems, this task is significantly more challenging and as of yet unexplored. A comparative study of two methods for solving this problem is presented in this paper. The eye corners detected by the two methods are then used for the pre-alignment and biometric performance evaluation experiments. The system utilising image pre-alignment is benchmarked against a baseline iris recognition system on the iris subset of the BioSecure database. In the benchmark, the workload associated with alignment compensation is significantly reduced, while the biometric performance remains unchanged or even improves slightly.

Contents

1 Introduction

The iris is one of the main biometric characteristics used in biometric systems around the world. At the time of this writing, the Indian Aadhaar system has enrolled over 1 billion subjects' multi-modal (including iris) biometric data [1]. The border control system of United Arab Emirates checks every traveller against a growing blacklist consisting of hundreds of thousands of subjects [2]. The deployments of this size and importance face strenuous requirements in terms of, among other matters, biometric performance and computational efficiency.

Following Daugman's approach [3], which is the core of most public operational systems, four major modules constitute an iris recognition system: (1) acquisition of the near-infrared image, where most current deployments require subjects to fully cooperate with the capture device in order to capture images of sufficient quality; (2) pre-processing, which involves a detection of inner and outer iris boundaries, a detection of eyelids, an exclusion of eyelashes as well as contact lens rings, a scrubbing of specular reflections and an estimation of quality factors [4]. Subsequently, the iris is mapped to dimensionless coordinates, i.e. a normalized rectangular texture, and an according noise mask is stored; (3) feature extraction, in which a two-dimensional binary feature vector, i.e. iris-code, is generated by applying adequate filters to the pre-processed iris texture. This binary data representation enables compact storage and rapid (4) comparison, which is based on the estimation of Hamming distance (*HD*) scores between pairs of iris-codes. In the comparison stage circular bit shifts are applied to iris-codes and *HD* scores are estimated at $\pm K$ different shifting positions, i.e. relative tilt angles, in order to compensate the biometric sample misalignment. The minimal obtained *HD*, which corresponds to an optimal alignment, represents the final score.

Considering multiple shifting positions during a template comparison increases the computational workload of the system and the probability of a false match with K [5]. This is especially important for identification systems, where an exhaustive search of the reference database is performed during an authentication attempt. By pre-aligning the eye images, the aforementioned cost (in terms of computational workload and biometric performance degradation) could be significantly reduced, thus partially alleviating the issues created by the necessity of alignment compensation. For the biometric references, the pre-alignment could be performed at enrollment stage, while any additional computational cost of pre-alignment of the biometric probes would be inconsequential in relation to the template comparison costs, since in any sizeable biometric identification system, the computational costs are dominated by the template comparisons [6]. Although image pre-alignment has been utilised in, for instance, fingerprint and face based biometric systems (see e.g. [7] and [8]), as of yet it has not been explored in the context of iris recognition systems.

The remainder of this paper is organised as follows: In section 2, the related work is presented. Section 3 explains the usage of eye corners in eye images pre-alignment and outlines the proposed approaches to automatic detection of eye corners in near-infrared images. The experimental set-up and obtained results are presented and discussed in section 4, while concluding remarks are given in section 5.

2 Related Work

The work presented in this paper combines two areas of research - automatic detection of eye corners and reduction of the alignment costs in iris identification systems. This section is accordingly divided into two subsections.

2.1 Eye Corner Detection

Facial landmark detection represents a well-studied area in computer vision. It forms the basis for numerous types of applications, such as face recognition or emotion estimation. Facial landmarks detected by state-of-the-art methods tend to vary in number and type; however, the vast majority of approaches extracts eye corner positions as specified in ISO/IEC 19794-5 [9].

In the context of iris recognition, automatic eye corner detection approaches for visible spectrum images have been presented by a number of researchers. Xu *et al.* [10] base their approach on the semantic features of the inner and outer eye corners, an angle model based on the eyelids and utilise a logistic regression classifier for the detection. Xia and Yan [11] use weighted variance projection function to detect first the regions of interest and then the eye corners themeselves. Erdogmus and Dugelay [12] use the Hough transform to detect the eyelid contours and subsequently establish the eye corners at the intersection of polynomials fitted to said contours. Santos and Proença [13] perform experiments on low-quality data, in which they utilise sclera segmentation and eyelid contours to generate a set of candidate points, from which the final eye corner locations are chosen based on a fusion of a number of metrics calculated for all the points in the candidate set. More recently, Zhang *et al.* [14] used a two-step process in which the rough locations of the eye corners are estimated and refined using image texture information.

All of the above report excellent results, ranging between 90% and 100% correct detection of eye corners - depending on how the groundtruth was established and what metrics and parameters were used to measure the detection accuracy. However, it is important to reiterate, that all of the mentioned approaches use *visible wavelength* eye images (or regions of interest extracted from facial images). Eye corner detection in *near-infrared* images, which are currently used in operational (large-scale) iris recognition systems, is a significantly more challenging task. In contrast to iris images acquired at visible wavelengths, near-infrared images exhibit a low contrast between sclera and skin, cf. figure 4. Hence, a proper sclera segmentation, which is required in some of the mentioned approaches, is not feasible for near-infrared images.

2.2 Alignment Cost Reduction

As has been mentioned in section 1, the traditional iris-code based iris identification systems require significant workload to be put into alignment compensation. In recent years, some interest has been exhibited towards developing methods to reduce (or even eliminate) the number of relative alignment positions that need to be considered in order to achieve an acceptable biometric performance. Du *et al.* [15] have presented a feature extractor for iris recognition based on one-dimensional signatures and showed that such an approach does not require an alignment of extracted templates. Alonso-Fernandez *et al.* [16] suggested to apply scale invariant feature transform to extract iris texture features prior to the normalisation step, where a comparison of keypoint-based feature vectors does not require the traditional alignment procedure. A partial alignment-compensating representation of the commonly used iris-code matrix was proposed by Rathgeb and Busch [17]. However, published rotation-invariant feature representations either require a more complex comparison process or reveal unpractical biometric performance. In the latter case, these may still be applied in a pre-selection step of a biometric identification scenario, see e.g. work of Konrad *et al.* [18]. Recently, Rathgeb *et al.* [19] introduced a method based on an analysis of the nature of iris-code and comparison scores between those. In a two-step process, the number of relative positions that need to be considered for two biometric samples was significantly decreased.

3 Proposed Methods

In this paper, two methods for eye corner detection in near-infrared eye images are presented. Before describing these, a brief outline of how the eye corners are used to pre-align an eye image is given below. Based on the two – left (L) and right (R) – eye corner points, the angle of a line through the two points is calculated as shown in equation 1.

$$\angle(L, R) = \arctan\left(\frac{R_y - L_y}{R_x - L_x}\right). \tag{1}$$

The image is rotated by the given angle, such that a line drawn between L and R is horizontal. The image is subsequently cropped in order to remove boundary artefacts resulting from the rotation. Those artefacts generate strong edges, which might negatively influence the segmentation process. The center of rotation C, which serves as the center of the cropped area, is based on the corner points as well:

$$C_x = \frac{L_x + R_x}{2}, C_y = \frac{L_y + R_y}{2}. \tag{2}$$

The size of the cropped image is set to 512×400 pixels. Figure 1 shows the eye corner landmarks, the line between the landmarks and the framing of the resulting cropping and rotation. As can be seen in the image, the inner eye corner is hard to define due to missing color information.

This method of absolute image pre-alignment is used with the eye corner locations produced with the methods outlined in following subsections. Note, that the aim is to align iris images prior to the segmentation stage. Alternatively, eye corners could be detected as part of the segmentation process, which might allow for an application of geometrical constraints, e.g. based on the detected pupil center.

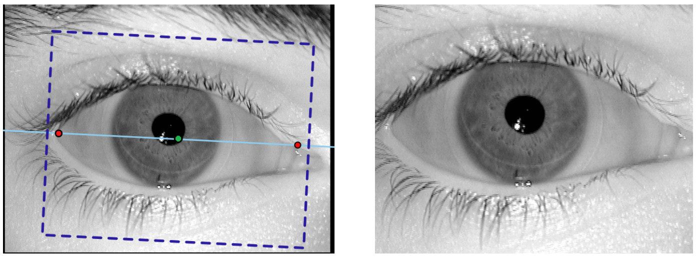

(a) (b)

Figure 1: Iris image with eye corner landmarks (red), the rotation center (green), the horizon line and the frame for cropping and rotation (a) as well as the resulting image (b).

3.1 Adapting Facial Landmark Detectors (FaceLD)

There exist many facial landmark detectors, which are made available in open-source toolboxes, e.g. dlib [20] and Bob [21] with menpofit [22], which were used in experiments performed for this paper. Those frameworks include pre-trained machine learning models, which are capable of detecting a large number of specific landmarks on a human face, among which are the eye corners. Naturally, these systems require an entire or at least a large part of a face to be present in an image. The eye images captured for the iris recognition systems only include a small part of the periocular area or are cropped (those two image formats are standardised by ISO/IEC 19794-6 [23]). A surprisingly effective idea is to utilise a high quality, noiseless facial image and insert the eye images into it, as shown in figure 2, so that the left and right face halves together with the inserted eye images are mirror reflections of each other. As an optional post-processing step, a semi-transparent smoothing transformation can be applied along the borders of the eye images. The two methods of inserting the eye image into the face image are referred to as *basic* (2a) and *smooth* (2b). The facial landmarks are then detected, as with processing a normal face image; the landmark positions from the left and right side of the face are averaged, expecting more robustness. The last step is to translate the eye corners positions from the coordinate system of the face image to that of the eye image and use them in the pre-alignment experiments.

3.2 Landmark Detection for Eye Images (EyeLD)

A logical next step is to train a model dedicated for eye images alone. The open-source dlib package [20] implements a landmarking model presented by Kazemi and Sullivan [24], which relies on an ensemble of randomized regression trees. For the training, a groundtruth of 9 landmarks marked by a single operator is used; it contains the eye corners themselves, pupil center and points along the lower and upper eyelid arches, as shown in figure 3. In the pre-alignment experiments, the detected eye corners are used directly or computed using the intersection between the polynomials or circles fitted (least-squares sense) to the eyelid landmarks.

(a) Eye image plainly inserted upon the facial image.

(b) A semi-transparent transform applied around the eye image edges.

Figure 2: Insertion of an iris image to a high resolution frontal face image.

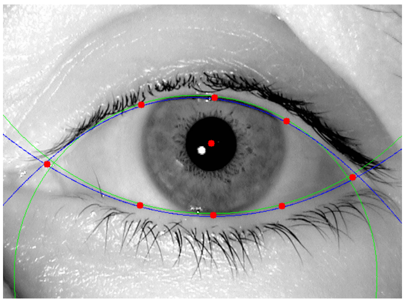

Figure 3: The 9 landmarks automatically detected by the model on a sample image. The curves show locating the eye corners by fitting circles (green) and polynomials (blue) to the eyelid landmarks.

4 Results

The evaluation of the proposed approaches is focused on following matters:

Biometric performance By pre-aligning the images, the number of shifting positions considered at the comparison stage is changed. This obviously affects the biometric performance of the system, which is evaluated by calculating the equal-error rate (EER) and the false non-match rate measured at false match rate of 0.01% ($\text{FNMR}_{0.01}$). We are interested in the minimum EER found and also define diminishing returns (DR) of the EER, where we allow the EER to be up to 10% over the minimum EER. This usually results in a drastically reduced remaining rotation. The cause for this are the outliers, which allow to slightly improve the EER at a much higher cost of alignment compensation.

Workload The required alignment compensation ($\pm K$) after the pre-alignment step.

Pre-alignment accuracy How far are the results yielded by the pre-alignment step from the objectively optimal alignment.

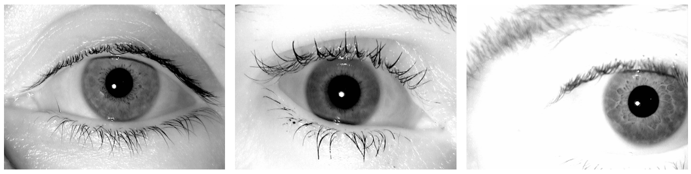

Figure 4: Example images from the BioSecure database.

Table 1: Baseline and groundtruth results (in %).

Method		Minimum			DR		
		K	EER	$\text{FNMR}_{0.01}$	K	EER	$\text{FNMR}_{0.01}$
Baseline		± 20	2.506	4.296	± 10	2.705	4.795
Groundtruth	Eye corners	± 7	2.148	3.690	± 5	2.336	4.288
	Polynomial fitting	± 5	2.188	3.496	± 3	2.347	4.171
	Circle fitting	± 15	2.347	3.699	± 5	2.506	4.178

The dataset chosen for the evaluation of the proposed approaches is the iris subset of the BioSecure database [25]. It contains 1680 left and right eye images from 210 subjects; the images of size 640×480 pixels were captured using a near-infrared camera. Most of the publicly available iris datasets come in the cropped image format, which makes them unsuitable for our experiments; the images in the BioSecure dataset are uncropped. Additionally, the quality of images varies in terms of eye position, rotation and illumination conditions, as shown in figure 4. For the model training (see subsection 3.2), the dataset is divided into 5 subsets, each containing 1344 training images and 336 test images. This allows to generate landmarks for the whole dataset, while ensuring that the training and test sets are always disjoint.

In the employed iris recognition system, the iris of a given sample image is detected and transformed to a normalised rectangular texture of 512×64 pixels. The normalised iris texture is divided into texture stripes to obtain 10 one-dimensional signals, each one averaged from adjacent texture rows. A row-wise convolution with a Log-Gabor wavelet is performed on each signal and the two bits of phase information are used to generate a 512×20 bits iris-code. During alignment compensation, the rotation per bit corresponds to $\frac{360}{512} \approx 0.7°$. We have employed the algorithm that was made available in [26] and described in detail in [27]. For the biometric performance evaluation, all possible template comparisons are considered. This results in a total of 2520 genuine comparisons and almost 1.4 million impostor comparisons. It should, however, be noted, that the results presented in the following sections can be achieved irrespective of the chosen feature extraction algorithm.

4.1 Baseline and Groundtruth

First, in order to create a reference point for the proposed methods, baseline and groundtruth results are established. The *baseline* is a normal, iris-code based system, which performs $K = \pm 24$ bit shifts during a template comparison. The *groundtruth* consists of the manually marked landmark types shown in figure 3; the eye corners for pre-alignment calculations are used directly or computed as the intersection of polynomials or circles fitted to eyelid landmarks. Those results are listed in table 1.

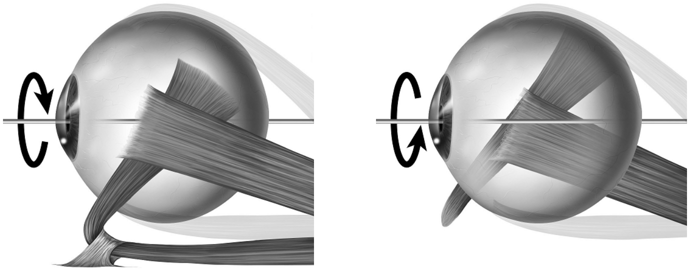

Figure 5: Eye with muscles responsible for torsional movement in the eye socket highlighted. Images by Patrick J. Lynch, medical illustrator (CC BY 2.5).

When benchmarked against the baseline system, the proposed pre-alignment technique allows to significantly reduce the required remaining alignment compensation (K). This verifies the conceptual soundness of the approach with manually marked landmark points. The diminishing returns (DR) allows for a trade-off between biometric performance improvement and workload reduction. As can be seen in table 1, the diminishing returns EER for the groundtruth is the same (or better) as for the baseline with full alignment compensation (minimum EER). In other words, by pre-aligning the samples, the required workload can be dramatically decreased without negatively affecting the biometric performance of the system.

It is also important to address, why the pre-alignment does not fully eliminate the need for further alignment compensation at the iris-code template comparison stage, i.e. why $K \neq 0$. This remaining rotation of up to $\pm 7\text{Bit} \approx \pm 4.92°$ is to be expected, since landmarks from the periocular region and not from the eye itself are used. The eye can rotate in the eye socket; this includes torsional movement induced by the superior/inferior rectus and superior/inferior oblique muscles [28] (see figure 5), with a range of motion that is "generally limited to angles of less than 10°" [29]. In recent years, methods for eye alignment during refractive surgery have been developed [30]. While extremely accurate, they depend on either continuous, active tracking (video) or static tracking based on a set of points marked in a reference image. The methods presented in this paper, however, perform the pre-alignment based on a single sample image.

4.2 Algorithmic Landmark Detection

Figure 6 shows various example images with landmarks detected by the proposed approaches marked. The results for the biometric performance and workload evaluation of the two approaches (subsections 3.1 and 3.2) are shown in table 2 and figure 7. Of interest are the benchmark against the baseline, i.e. by how much K decreased in an automated setting and the benchmark against the groundtruth (especially in case of EyeLD), i.e. by how much the automated approaches could still be improved.

For both approach classes, we observe an improvement over the baseline in both the minimum and diminishing returns EER setting. In all cases (except for circle fitting), K is significantly reduced (up to being halved), while the biometric performance in terms of EER and $\text{FNMR}_{0.01}$ remains unchanged or is improved. The FaceLD approach based on the Bob framework [21] and menpofit [22] model performs well. The model offered by the dlib [20] package was also tried, but was left out due to very poor results. The smoothing transform around the eye image edges in FaceLD approach performs worse than the basic version of FaceLD approach. This could be due to the eye corners being blurred out when they are located near the border of the eye image. Thus, potentially a more sophisticated approach would have to be applied. In terms of alignment workload reduction, the FaceLD approaches outperform the EyeLD approaches. On the other hand, the biometric performance of EyeLD approaches is bet-

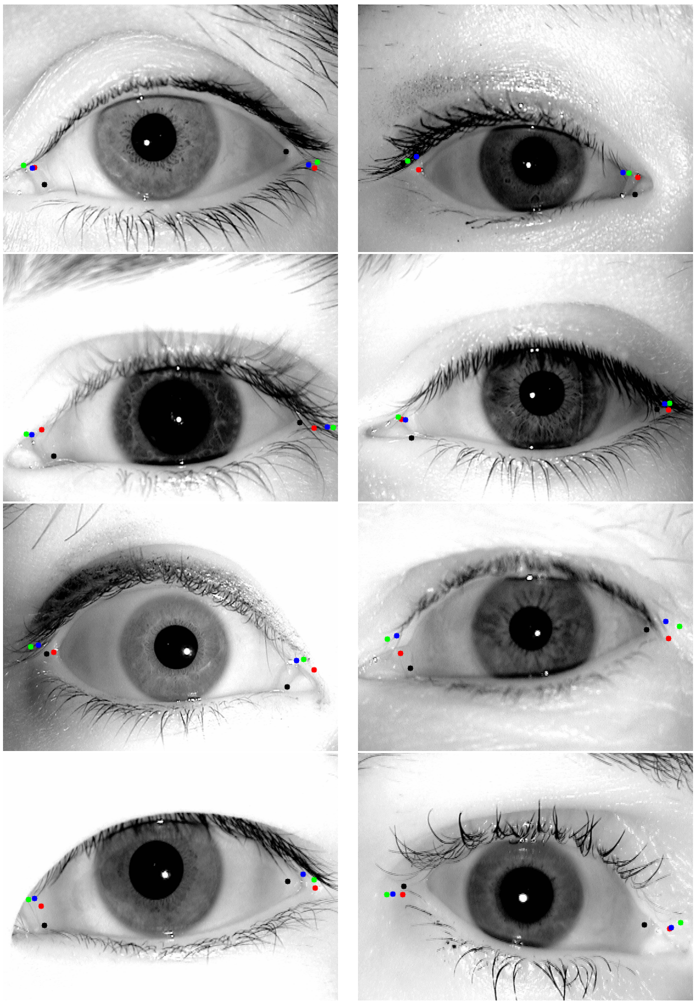

Figure 6: Example images with landmarks detected by the proposed approaches: FaceLD - basic (black), EyeLD - Corners (red), EyeLD - Polynomial (green), EyeLD - Circle (blue).

Table 2: Algorithmic results.

Method		Minimum			DR		
		K	EER	$\text{FNMR}_{0.01}$	K	EER	$\text{FNMR}_{0.01}$
FaceLD	Basic	±10	2.589	3.961	±6	2.748	4.625
	Smooth	±12	2.665	4.280	±7	2.864	4.654
EyeLD	Eye corners	±13	2.352	4.027	±11	2.467	4.142
	Polynomial fitting	±17	2.193	3.558	±12	2.313	3.868
	Circle fitting	±23	2.396	3.836	±11	2.592	4.214

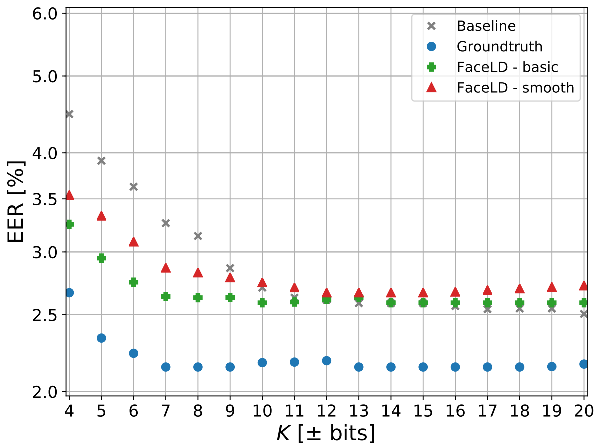

(a) Adaptation of facial landmarks detection.

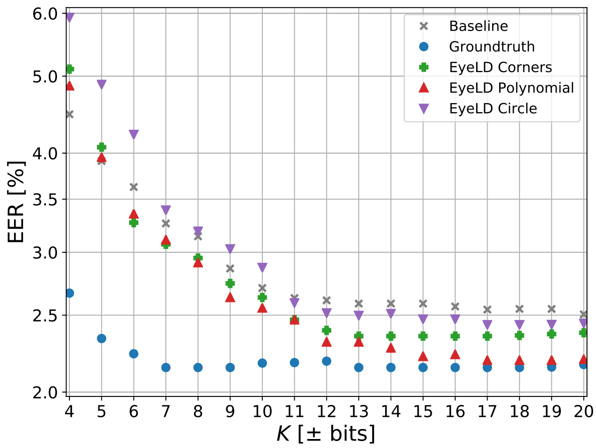

(b) Dedicated eye landmarks detection.

Figure 7: Biometric performance comparison for the evaluated approaches (note the logarithmic scale of the y-axis).

Table 3: Parameters of the impostor scores distributions.

K	0	1	2	3	4	8	16	24
mean	0.498	0.495	0.492	0.489	0.486	0.478	0.469	0.466
st. deviation	0.024	0.023	0.023	0.022	0.021	0.018	0.016	0.014
skewness	-0.026	-0.034	-0.052	-0.083	-0.127	-0.351	-0.598	-0.717
ex. kurtosis	0.291	0.378	0.466	0.550	0.650	1.202	2.225	2.842

ter than both the FaceLD approaches and the baseline. It is also worth noting, that while in terms of K reduction, the EyeLD approaches do not match the results achieved by the groundtruth, one could safely assume that with a large enough training corpus, the results of the groundtruth and the automated method would converge. One idea for future work is to mirror and rotate the available images in each training set fold, thus dramatically enlarging the training set and thereby the landmark detection accuracy.

Figure 8 shows a cumulative distribution of the distance from optimal alignment after the pre-alignment step performed by the proposed approaches. For example, it can be seen, that after a pre-alignment step around 80% of the images are less

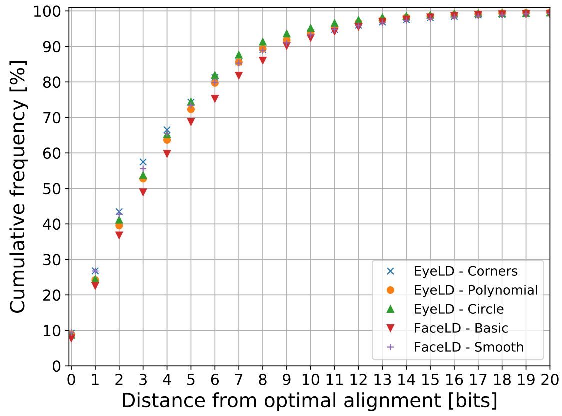

Figure 8: Cumulative distributions of the distance from the optimal alignment achieved by the presented pre-alignment approaches.

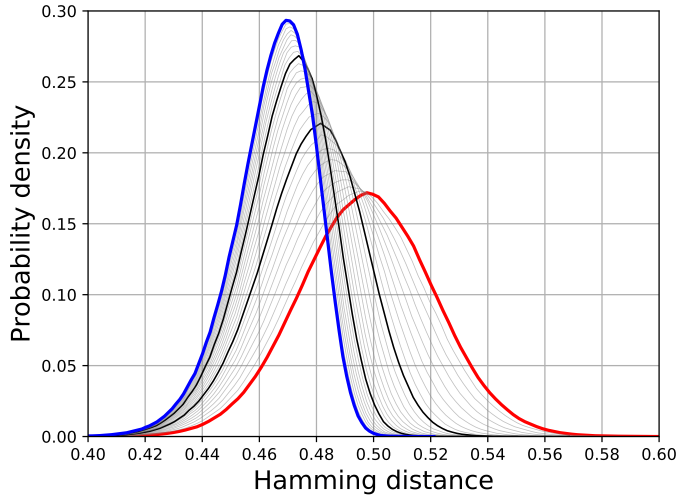

Figure 9: Kernel density estimate of impostor scores from no (red) to $K = \pm 24$ bits (blue) rotation compensation.

than 8 bits from the optimal alignment. Note, that this figure does not necessarily reflect the EER scores, since optimal alignment is not a guarantee for an optimal score (bad quality images can have a high *HD* score even at the optimal alignment position). In other words, the distance from the optimal alignment would only be a good predictor of biometric performance, if and only if the quality of images (apart from rotational variation) was very high.

While the pre-alignment is not expected to have a significant positive impact on the genuine scores, it affects the impostor scores significantly. As can be seen in figure 9 and table 3, when no alignment compensation is applied (i.e. $K = 0$), the impostor scores approximate a normal distribution around $HD = 0.5$. However, with the growing K value, the distribution moves towards left (i.e. towards genuine scores distribution). As has been mentioned in section 1, this increases the probability of false positives due to larger overlap between the genuine and impostor distributions. By pre-aligning and decreasing K, this effect is counteracted, thereby slightly improving the biometric performance in addition to reducing the workload.

5 Conclusion

In this paper, a software-based approach to alignment cost reduction in iris recognition systems has been introduced. Experiments conducted on the iris subset of the BioSecure database have lead to following key findings:

- Pre-alignment improves the biometric performance in terms of EER and $\mathrm{FNMR}_{0.01}$ when benchmarked against a baseline system.
- Pre-alignment reduces the required alignment compensation workload in terms of K when benchmarked against a baseline system.
- Proposed landmark detection approaches work, but as the groundtruth experiments demonstrate, there is still room for improvement.

While there exists a number of approaches for automatic corner detection in visible spectrum images, the authors are not aware of such work in the near-infrared spectrum. In this paper, two methods for achieving this task were presented with the resulting landmarks used for image pre-alignment. In addition to eye landmark detection accuracy refinement, a potentially interesting area for future work is investigating the possibility of application of the presented approaches to cropped eye images, as defined in ISO/IEC 19794-6 [23]. It is worth noting, that many areas of biometric research could benefit from iris image pre-alignment. This pertains in particular to privacy-enhancing technologies, i.e. biometric template protection [31], in which comparisons are performed in an encrypted domain, such that a proper alignment is (in many cases) not feasible.

Acknowledgment

This work was partially supported by the German Federal Ministry of Education and Research (BMBF), as well as by the Hessen State Ministry for Higher Education, Research and the Arts (HMWK) within Center for Research in Security and Privacy (CRISP) and by the Austrian Science Fund (FWF), project no. P27776. This work was partially supported by the Austrian Science Fund, project no. P27776.

References

[1] Unique Identification Authority of India (UIDAI), *Aadhaar issued summary*, https://portal.uidai.gov.in/uidwebportal/dashboard.do, 2010 (cit. on p. 2).

[2] A. N. Al-Raisi and A. M. Al-Khouri, "Iris recognition and the challenge of homeland and border control security in UAE," *Telematics and Informatics*, vol. 25, no. 2, pp. 117–132, 2008 (cit. on p. 2).

[3] J. Daugman, "How iris recognition works," *IEEE Trans. on Circuits and Systems for Video Technology*, vol. 14, no. 1, pp. 21–30, Jan. 2004 (cit. on p. 2).

[4] ISO/IEC JTC1 SC37 Biometrics, *Iso/iec 29794-6:2015. information technology – biometric sample quality – part 6: Iris image data*, International Organization for Standardization and International Electrotechnical Committee, Jul. 2015, p. 29 (cit. on p. 2).

[5] J. Daugman, "Information theory and the IrisCode," *IEEE Trans. on Information Forensics and Security*, vol. 11, no. 2, pp. 400–409, Feb. 2016 (cit. on p. 2).

[6] F. Hao, J. Daugman, and P. Zielinski, "A fast search algorithm for a large fuzzy database," *IEEE Trans. on Information Forensics and Security*, vol. 3, no. 2, pp. 203–212, Jun. 2008, ISSN: 1556-6013 (cit. on p. 2).

[7] B. Tams, "Absolute fingerprint pre-alignment in minutiae-based cryptosystems," in *Intl. Conf. of the BIOSIG Special Interest Group (BIOSIG)*, Sep. 2013, pp. 1–12 (cit. on p. 2).

[8] X. Cao, Y. Wei, F. Wen, and J. Sun, "Face alignment by explicit shape regression," *Intl. Journal of Computer Vision*, vol. 107, no. 2, 2014 (cit. on p. 2).

[9] ISO/IEC JTC1 SC37 Biometrics, *ISO/IEC 19794-5:2011. information technology – biometric data interchange formats – part 5: Face image data*, International Organization for Standardization and International Electrotechnical Committee, Oct. 2011, p. 120 (cit. on p. 2).

[10] C. Xu, Y. Zheng, and Z. Wang, "Semantic feature extraction for accurate eye corner detection," in *2008 19th Intl. Conf. on Pattern Recognition*, Dec. 2008, pp. 1–4 (cit. on p. 2).

[11] H. Xia and G. Yan, "A novel method for eye corner detection based on weighted variance projection function," in *2009 2nd Intl. Congress on Image and Signal Processing*, Oct. 2009, pp. 1–4 (cit. on p. 2).

[12] N. Erdogmus and J.-L. Dugelay, "An efficient iris and eye corners extraction method," in *Structural, Syntactic, and Statistical Pattern Recognition: Joint IAPR Intl. Workshop*, Springer, 2010, pp. 549–558 (cit. on p. 2).

[13] G. Santos and H. Proença, "A robust eye-corner detection method for real-world data," in *2011 Intl. Joint Conf. on Biometrics (IJCB)*, Oct. 2011, pp. 1–7 (cit. on p. 2).

[14] Z. Zhang, Y. Shen, W. Lin, and B. Zhou, "Eye corner detection with texture image fusion," in *2015 Asia-Pacific Signal and Information Processing Association Annual Summit and Conference (APSIPA)*, Dec. 2015, pp. 992–995 (cit. on p. 2).

[15] Y. Du, R. W. Ives, D. M. Etter, and T. B. Welch, "Use of one-dimensional iris signatures to rank iris pattern similarities," *Optical Engineering*, vol. 45, no. 3, Mar. 2006 (cit. on p. 3).

[16] F. Alonso-Fernandez, P. Tome-Gonzalez, V. Ruiz-Albacete, and J. Ortega-Garcia, "Iris recognition based on SIFT features," in *2009 First IEEE Intl. Conf. on Biometrics, Identity and Security (BIdS)*, 2009, pp. 1–8 (cit. on p. 3).

[17] C. Rathgeb and C. Busch, "Comparing binary iris biometric templates based on counting bloom filters," in *Proc. 18th Iberoamerican Congress on Progress in Pattern Recognition, Image Analysis, Computer Vision, and Applications (CIARP)*, 2013 (cit. on p. 3).

[18] M. Konrad, H. Stögner, A. Uhl, and P. Wild, "Computationally efficient serial combination of rotation-invariant and rotation compensating iris recognition algorithms," in *Proceedings of the Intl. Conf. on Computer Vision Theory and Applications (VISIGRAPP 2010)*, 2010, pp. 85–90 (cit. on p. 3).

[19] C. Rathgeb, H. Hofbauer, A. Uhl, and C. Busch, "Triplea: Accelerated accuracy-preserving alignment for iris-codes," in *2016 Intl. Conf. on Biometrics (ICB)*, Jun. 2016, pp. 1–8 (cit. on p. 3).

[20] D. E. King, "Dlib-ml: A machine learning toolkit," *Journal of Machine Learning Research*, vol. 10, no. Jul, pp. 1755–1758, 2009 (cit. on pp. 3, 5).

[21] A. Anjos, L. E. Shafey, R. Wallace, M. Günther, C. McCool, and S. Marcel, "Bob: A free signal processing and machine learning toolbox for researchers," in *20th ACM Conf. on Multimedia Systems (ACMMM), Nara, Japan*, ACM Press, Oct. 2012 (cit. on pp. 3, 5).

[22] J. Alabort-i-Medina, E. Antonakos, J. Booth, P. Snape, and S. Zafeiriou, "Menpo: A comprehensive platform for parametric image alignment and visual deformable models," in *Proceedings of the 22nd ACM Intl. Conf. on Multimedia*, ser. MM '14, ACM, 2014, pp. 679–682 (cit. on pp. 3, 5).

[23] ISO/IEC JTC1 SC37 Biometrics, *ISO/IEC 19794-6:2011. information technology – biometric data interchange formats – part 6: Iris image data*, International Organization for Standardization and International Electrotechnical Committee, Oct. 2011, p. 19 (cit. on pp. 3, 7).

[24] V. Kazemi and J. Sullivan, "One millisecond face alignment with an ensemble of regression trees," in *2014 IEEE Conf. on Computer Vision and Pattern Recognition*, Jun. 2014, pp. 1867–1874 (cit. on p. 3).

[25] J. Ortega-Garcia, J. Fierrez, F. Alonso-Fernandez, J. Galbally, M. R. Freire, *et al.*, "The multiscenario multienvironment BioSecure multimodal database (BMDB)," *IEEE Trans. on Pattern Analysis and Machine Intelligence*, vol. 32, no. 6, pp. 1097–1111, Jun. 2010, ISSN: 0162-8828 (cit. on p. 4).

[26] *USIT – University of Salzburg iris toolkit*, http://www.wavelab.at/sources/Rathgeb16a, Version 2.0.x (cit. on p. 4).

[27] C. Rathgeb, A. Uhl, and P. Wild, *Iris Recognition: From Segmentation to Template Security*, ser. Advances in Information Security. Springer Verlag, 2013, vol. 59 (cit. on p. 4).

[28] D. L. Sparks, "The brainstem control of saccadic eye movements," *Nature Reviews Neuroscience*, vol. 3, no. 12, pp. 952–964, 2002 (cit. on p. 5).

[29] L. R. Young and D. Sheena, "Survey of eye movement recording methods," *Behavior Research Methods & Instrumentation*, vol. 7, no. 5, pp. 397–429, 1975, ISSN: 1554-3528 (cit. on p. 5).

[30] K. Holmqvist, M. Nyström, R. Andersson, R. Dewhurst, H. Jarodzka, and J. Van de Weijer, *Eye tracking: A comprehensive guide to methods and measures*. OUP Oxford, 2011 (cit. on p. 5).

[31] K. Nandakumar and A. K. Jain, "Biometric template protection: Bridging the performance gap between theory and practice," *IEEE Signal Processing Magazine - Special Issue on Biometric Security and Privacy*, pp. 1–12, 2015 (cit. on p. 7).